W. *Inorg. Chim. Acta* **1978**, *29*, L203.
(7) Hieber, W.; Kruck, T. *Chem. Ber.* **1962**, *95*, 2027.
(8) Dance, N. S.; Jones, C. H. W. *J. Organomet. Chem.* **1978**, *152*, 175.
(9) Chia, L. Y.; McWhinnie, W. R. *J. Organomet. Chem.* **1978**, *148*, 165.
(10) Livingstone, S. E. *Q. Rev., Chem. Soc.* **1965**, *19*, 386.
(11) Cross, R. J.; Green, T. H.; Keat, R. *J. Chem. Soc., Dalton Trans.* **1976**, 382, 1486.
(12) Goggin, P. L.; Goodfellow, R. J.; Haddock, S. R. *J. Chem. Soc., Chem. Commun.* **1975**, 176.
(13) Cross, R. J.; Green, T. H.; Keat, R.; Paterson, J. F. R. *Inorg. Nucl. Chem. Lett.* **1975**, *11*, 145.
(14) Fergusson, J. E.; Loh, K. S. *Aust. J. Chem.* **1973**, *26*, 2615.
(15) Good, R.; Merbach, A. E. *Helv. Chim. Acta* **1974**, *57*, 1192.
(16) Piraino, P.; Faraone, F.; Pietropaolo, R. *Peloritana Pericolanti, Cl. Sci. Fis., Mat. Natur. Atti Accad.* **1971**, *51*, 283; *Chem. Abstr.* **1973**, *79*, 13011.
(17) Allkins, J. R.; Hendra, P. J. *J. Chem. Soc. A* **1967**, 1325.
(18) Sato, M.; Yoshida, T. *J. Organomet. Chem.* **1973**, *51*, 231.
(19) Sato, M.; Yoshida, T. *J. Organomet. Chem.* **1974**, *67*, 395.
(20) Sato, M.; Yoshida, T. *J. Organomet. Chem.* **1975**, *87*, 217.
(21) Mohr, D.; Wienand, H.; Ziegler, M. L. *J. Organomet. Chem.* **1977**, *134*, 281.
(22) Sato, M.; Yoshida, T. *J. Organomet. Chem.* **1975**, *94*, 403.
(23) Kharasch, M. S.; Seyler, R. C.; Mayo, F. R. *J. Am. Chem. Soc.* **1938**, *60*, 882.
(24) DeStefano, N. J.; Burmeister, J. L. *Synth. React. Inorg. Met.-Org. Chem.* **1977**, *3*, 313.
(25) Ramsay, D. A. *J. Am. Chem. Soc.* **1952**, *74*, 72.
(26) Ahmed, F. R. NRC-10, National Research Council of Canada, Ottawa, 1970.
(27) "International Tables for X-Ray Crystallography"; Kynoch Press: Birmingham, England, 1974; Vol. IV, Chapter 2.
(28) Reference 3, p 137.
(29) Gysling, H. J., unpublished work.
(30) Davidson, P. J.; Lappert, M. F.; Pearce, R. *Acc. Chem. Res.* **1974**, *7*, 209.
(31) Collier, M. R.; Kingston, B. M.; Lappert, M. F. U.S. Patent 3 763 197, 1973.
(32) Hamada, K.; Morishita, H. *Synth. React. Inorg. Met.-Org. Chem.* **1977**, *7*, 355.
(33) McAuliffe, C. A.; Niven, I. E.; Parish, R. V. *Inorg. Chim. Acta* **1977**, *22*, 239.
(34) Burmeister, J. L. In "Chemistry and Biochemistry of Thiocyanic Acid and Its Derivatives"; Newman, H. A., Ed.; Academic Press: London, 1975; Chapter 2, pp 68–130.
(35) Anderson, S. J.; Norbury, A. H. *J. Chem. Soc., Chem. Commun.* **1975**, 48.
(36) Kargol, J. A.; Crecely, R. W.; Burmeister, J. L. *Inorg. Chim. Acta* **1977**, *25*, L109.
(37) Cheng, C. P.; Brown, T. L.; Fultz, W. C.; Burmeister, J. L. *J. Chem. Soc., Chem. Commun.* **1977**, 599.
(38) Johnson, C. K. "ORTEP-II", Report ORNL-3794, 2nd revision; Oak Ridge National Laboratory: Oak Ridge, Tenn., 1971.
(39) Cotton, F. A.; Wilkinson, G. "Advanced Inorganic Chemistry", 2nd ed.; Interscience: New York, 1966.
(40) Pearson, R. G. *Science* **1966**, *151*, 172. *J. Chem. Educ.* **1968**, *45*, 581, 643.
(41) Palenik, G. J.; Mathew, M.; Steffen, W. L.; Beran, G. *J. Am. Chem. Soc.* **1975**, *97*, 1059.
(42) Gillespie, R. J.; Nyholm, R. S. *Q. Rev., Chem. Soc.* **1957**, *11*, 339. Gillespie, R. J. *J. Chem. Educ.* **1970**, *47*, 18.
(43) Pauling, L. "The Nature of the Chemical Bond", 3rd ed.; Cornell University Press: Ithaca, NY, 1960.
(44) Skakke, P. E.; Rasmussen, S. E. *Acta Chem. Scand.* **1970**, *24*, 2634.
(45) Beran, G.; Carty, A. J.; Chieh, P. C.; Patel, H. A. *J. Chem. Soc., Dalton Trans.* **1973**, 488.
(46) Dewan, J.; Silver, J. *J. Organomet. Chem.* **1977**, *125*, 125; *J. Chem. Soc., Dalton Trans.* **1977**, 644; *Aust. J. Chem.* **1977**, *30*, 487; *Acta Crystallogr., Sect. B* **1977**, *33*, 1469.
(47) Pazdernik, L.; Brisse, F.; Rivest, R. *Acta Crystallogr., Sect. B* **1977**, *33*, 1780. Corey, E. R.; Corey, J. Y.; Paton, W. F.; Glick, M. D. *Ibid.* **1977**, *33*, 1254.

Contribution from the Department of Chemistry,
The University of Alberta, Edmonton, Alberta, Canada, T6G 2G2

Structure of $[Rh_2(CO)_2(\mu\text{-}Cl)((C_6H_5)_2PCH_2P(C_6H_5)_2)_2][BF_4]$. A Binuclear "A-Frame" Complex Showing the Open "Active" Site

MARTIN COWIE* and STEPHEN K. DWIGHT

Received April 17, 1979

The structure of the complex $[Rh_2(CO)_2(\mu\text{-}Cl)((C_6H_5)_2PCH_2P(C_6H_5)_2)_2][BF_4]$ has been determined by X-ray crystallography, verifying that it is an "A-frame" type species. The structural parameters are similar in most aspects to those of the closely related species $[Rh_2(CO)_2(\mu\text{-}S)((C_6H_5)_2PCH_2P(C_6H_5)_2)_2]$, with the significant difference that the "active" site, bridging the two metal centers, is more open to attack by small molecules in the present complex. The title complex crystallizes in the space group $C_i^1\text{-}P\bar{1}$ from an acetone solution containing as the only anions PF_6^- and $B(C_6H_5)_4^-$. Evidence suggests that the BF_4^- anion results from the leaching of boron from the glass by HF. The reduced unit cell has dimensions a = 13.044 (1) Å, b = 14.962 (2) Å, c = 12.800 (2) Å, α = 96.20 (1)°, β = 92.56 (1)°, and γ = 86.42 (1)° with Z = 2. On the basis of 5729 unique, observed reflections the structure was refined by full-matrix, least-squares techniques to agreement indices of R = 0.046 and R_w = 0.064. Some relevant metrical parameters are Rh–P(av) = 2.321 (2) Å, Rh–C = 1.794 (7) and 1.807 (7) Å, Rh–Cl = 2.380 (2) and 2.406 (2) Å, C–O = 1.184 (8) and 1.202 (8) Å, Rh–Rh = 3.1520 (8) Å, C–Rh–Cl = 170.9 (2) and 172.6 (3)°, and Rh–Cl–Rh = 82.38 (5)°.

Introduction

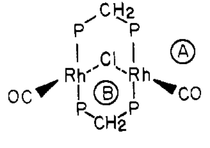

1

The reactions of small molecules with binuclear metal complexes and the subsequent coordination modes of these molecules are of considerable current interest owing to the obvious implications regarding homogeneous catalysis by metal systems.[1] As part of our continuing investigations in this area[2-6] we have been studying the chemistry of the binuclear cationic species $[Rh_2(CO)_2(\mu\text{-}Cl)(DPM)_2]^+$ (**1**),[7] assumed to be an "A-frame" type complex based on spectral data and the structural characterization of its carbonyl adduct $[Rh_2(CO)_2(\mu\text{-}CO)(\mu\text{-}Cl)(DPM)_2]^+$ (**2**).[2,3] The "A-frame" complex **1** reacts reversibly with CO[2,8] and SO_2[4,5,8] and undergoes facile reactions with several other small molecules, including NO, N_2Ph^+, CS_2,[9] and TCNE.[10] The reactions with CO and SO_2 contrast the two possible modes of attack of small molecules

0020-1669/79/1318-2700$01.00/0 © 1979 American Chemical Society

with complex **1**. Whereas CO attacks the open Rh coordination site (A) remote from the bridging site,[2,8] SO_2 seems to attack and coordinate directly at the proposed[11] "active" site—the bridging position (B).[5,8]

In a recent report on the closely related, sulfide-bridged, "A-frame" complex $[Rh_2(CO)_2(\mu\text{-}S)(DPM)_2]$ (**3**),[11] the "active" site was found to be effectively blocked, at least in the solid state, by four of the DPM phenyl groups. In particular, two rings were found to severely obstruct this site. Similarly, in the SO_2-bridged, "A-frame" complex $[Rh_2Cl_2(\mu\text{-}SO_2)(DPM)_2]$ (**4**),[4,5] the bridging coordination site is again effectively blocked by four phenyl groups and again two of these rings have particularly close contacts with the rhodium atoms. Although the details of the reactions of complex **3** with small molecules are not known to us, the SO_2-bridged species **4** is found to react in a manner which is consistent with attack at the sites remote from the bridging site,[5] implying that attack at the bridging site is hindered, even in solution.

Since complex **1** seems to allow attack both at the "active" site and at the site remote from the bridging position, it was of interest to us to obtain structural information on this "A-frame" species with hopes of gaining an insight into the modes of attack of small molecules with this species and of enabling us to understand more completely its chemistry. The X-ray structural determination of complex **1** was therefore undertaken.

Experimental Section

All solvents were appropriately dried and degassed prior to use and all reactions were carried out under an atmosphere of dinitrogen. Benzenediazonium hexafluorophosphate was purchased from Aldrich Chemicals, $NaBF_4$ and $NaPF_6$ were purchased from Alfa Products, and $[Rh_2(CO)_2(\mu\text{-}Cl)(DPM)_2][BPh_4]$[7] was prepared by the reported methods.[2,5] Infrared spectra were recorded on a Perkin-Elmer Model 467 spectrometer using Nujol mulls on KBr plates and NMR spectra were recorded on a Bruker HFX-90 NMR spectrometer.

Preliminary Crystallization of $[Rh_2(CO)_2(\mu\text{-}Cl)(DPM)_2][BF_4]$. To a solution of 0.100 g (0.072 mmol) of $[Rh_2(CO)_2(\mu\text{-}Cl)(DPM)_2]$-$[BPh_4]$ in 8 mL of acetone was added 0.020 g (0.080 mmol) of $[PhN_2][PF_6]$. Slow diffusion of diethyl ether into the reaction mixture yielded both yellow-orange and dark red prismatic crystals. Although too few of the yellow-orange crystals were obtained for elemental analysis, an infrared spectrum of the complex (ν(CO) 1995 (s), 1978 (vs) cm^{-1}; ν(BF) 1060 (m, br) cm^{-1}) indicated that it was the BF_4^- salt of the "A-frame" complex **1**.

Data Collection. A yellow-orange crystal of the title compound was mounted and sealed in a glass capillary tube. Preliminary film data showed $\bar{1}$ Laue symmetry and no systematic absences, consistent with the space groups $P1$ and $P\bar{1}$. The centrosymmetric space group was chosen and later verified by (1) the successful refinement of the structure with acceptable positional parameters, thermal parameters, and agreement indices and (2) the location of all hydrogen atoms in difference Fourier syntheses. Accurate cell parameters were obtained by a least-squares analysis of the setting angles of 12 carefully centered reflections chosen from diverse regions of reciprocal space (50° < 2θ < 70°, Cu Kα radiation) and obtained by using a narrow X-ray source (see Table I for pertinent crystal data). A cell reduction[12] failed to show the presence of higher symmetry. The reduced cell is reported.

Data were collected on a Picker four-circle automated diffractometer equipped with a scintillation counter and pulse-height analyzer, tuned to accept 90% of the Cu Kα peak. Background counts were measured at both ends of the scan range with stationary crystal and counter. The intensities of three standard reflections were measured every 100 reflections and four additional standards were measured three times a day. All standards remained constant to within 1.5% of the mean throughout the data collection.

The intensities of 7416 unique reflections (2° ≤ 2θ ≤ 120°) were measured by using Cu Kα radiation. Data were processed in the usual manner with a value of 0.05 for p.[13] Absorption corrections were applied to the data by using Gaussian integration.[14]

Structure Solution and Refinement. The positions of the two independent Rh atoms were obtained from a sharpened Patterson synthesis. Subsequent refinements and difference Fourier calculations led to the location of all other atoms. Atomic scattering factors were taken from Cromer and Waber's tabulations[15] for all atoms except hydrogen for which the values of Stewart et al.[16] were used. Anomalous dispersion terms[17] for Rh, Cl, P, and F were included in F_c. All carbon atoms of the phenyl rings were refined as rigid groups having D_{6h} symmetry and C–C distances of 1.392 Å. The hydrogen atoms were included as fixed contributions and were not refined. Their idealized positions were calculated from the geometries about their attached carbon atoms by using C–H distances of 0.95 Å. Hydrogen atoms were assigned isotropic thermal parameters of 1 $Å^2$ greater than their attached carbon atom. All other nongroup atoms were refined individually with anisotropic thermal parameters.

Table I. Summary of Crystal Data and Intensity Collection

compd	$[Rh_2(CO)_2(\mu\text{-}Cl)(DPM)_2][BF_4]$
formula	$C_{52}H_{44}B_1Cl_1F_4O_2P_4Rh_2$
formula wt	1152.89
a, Å	13.044 (1)
b, Å	14.962 (2)
c, Å	12.800 (2)
α, deg	96.20 (1)
β, deg	92.56 (1)
γ, deg	86.42 (1)
V, $Å^3$	2476.78
Z	2
density, g cm^{-3}	1.545 (calcd), 1.547 (5) (exptl by flotation)
space group	$C_i^1-P\bar{1}$
cryst dimens, mm	0.345 × 0.303 × 0.147
cryst vol, mm^3	0.0129
cryst shape	triclinic prism with faces of the form {001}, {110}, {011}, and {101}
temp, °C	20
radiation	Cu Kα (λ 1.540 562 Å) filtered with 0.5 mil thick nickel foil
μ, cm^{-1}	77.256
range in abs corr factors (as applied to F_o^2)	0.156–0.403
receiving aperture	4 mm × 4 mm, 30 cm from crystal
takeoff angle, deg	2.90
scan speed	2° in 2θ/min
scan range	0.80° below Kα_1 to 0.80° above Kα_2
bkgd counting time, s	10 ($3 \leqslant 2\theta \leqslant 75°$), 20 ($75 < 2\theta \leqslant 104°$), 40 ($104 < 2\theta \leqslant 120°$)
2θ limits	$3° \leqslant 2\theta \leqslant 120°$
final no. of variables	298
unique data used ($F_o^2 \geqslant 3\sigma(F_o^2)$)	5729
error in observn of unit wt	1.792
R	0.046
R_w	0.064

Although the infrared spectra of these crystals indicated that the present complex had crystallized as the BF_4^- salt, our initial unwillingness to accept the apparent transformation of PF_6^- and BPh_4^- into BF_4^- led us to attempt refinement of the electron density about the 1(c) and 1(f) inversion centers as PF_6^- anions. However, these refinement attempts proved unsuccessful, even considering disorder of these groups. The thermal parameters for both phosphorus atoms exceeded 30 $Å^2$ and chemically unreasonable P–F distances resulted. A closer inspection of the difference Fourier map indicated eight distinct peaks about both sets of inversion centers, corresponding to superimposed, inversion related, tetrahedral BF_4^- groups. In fact, the central peaks were more consistent with boron than phosphorus, having intensities (4.7 and 3.3 e/$Å^3$) comparable to the half-weighted fluorine peaks (3.7–1.8 e/$Å^3$). Refinement of this model as inversion disordered BF_4^- groups proceeded well, resulting in reasonable bond lengths, thermal parameters and well-defined tetrahedral geometries about the central boron atoms.

The final model with 298 parameters varied converged to $R = 0.046$ and $R_w = 0.064$.[18] In the final difference Fourier map all of the 20 highest peaks were in the vicinity of the phenyl rings (0.66–0.41 e/$Å^3$). A typical carbon atom on earlier syntheses had an electron density of about 5.0 e/$Å^3$. The final positional parameters of the group and nonhydrogen atoms are given in Tables II and III. The derived hydrogen positions and their thermal parameters, the root-mean-square

Table II. Positional and Thermal Parameters for the Nongroup Atoms of $[Rh_2(CO)_2(\mu\text{-}Cl)(DPM)_2][BF_4]$

atom	x[a]	y	z	U_{11}[b]	U_{22}	U_{33}	U_{12}	U_{13}	U_{23}
Rh(1)	0.40834 (3)	0.26969 (3)	0.12814 (3)	4.39 (3)	3.55 (3)	2.97 (2)	−0.60 (2)	0.40 (20)	0.16 (2)
Rh(2)	0.22996 (3)	0.13772 (3)	0.07315 (3)	3.50 (3)	4.43 (3)	2.83 (2)	−0.62 (2)	0.20 (2)	0.02 (2)
P(1)	0.3539 (1)	0.2916 (1)	0.2999 (1)	4.30 (9)	3.56 (8)	2.98 (7)	−0.28 (7)	0.24 (6)	0.20 (6)
P(2)	0.1866 (1)	0.1546 (1)	0.2482 (1)	3.84 (8)	3.97 (8)	3.02 (7)	−0.31 (6)	0.19 (6)	0.37 (6)
P(3)	0.4513 (1)	0.2486 (1)	−0.0471 (1)	3.76 (8)	4.04 (8)	3.41 (7)	−0.14 (7)	0.54 (6)	0.41 (6)
P(4)	0.2816 (1)	0.1132 (1)	−0.0994 (1)	3.56 (8)	4.34 (8)	3.03 (7)	−0.08 (7)	0.31 (6)	−0.02 (6)
Cl	0.4043 (1)	0.1092 (1)	0.1290 (1)	4.06 (8)	3.84 (8)	4.00 (7)	0.05 (6)	−0.07 (6)	0.38 (6)
O(1)	0.4525 (5)	0.4614 (4)	0.1349 (5)	12.0 (5)	4.9 (3)	7.0 (4)	−2.7 (3)	1.0 (3)	0.4 (3)
O(2)	0.0117 (4)	0.1436 (5)	0.0009 (5)	3.8 (3)	16.0 (6)	6.7 (4)	−0.9 (3)	−0.5 (3)	0.4 (4)
C(1)	0.4330 (6)	0.3875 (5)	0.1318 (5)	6.8 (5)	4.8 (4)	3.5 (3)	−1.4 (4)	0.9 (3)	−0.2 (3)
C(2)	0.0969 (6)	0.1438 (6)	0.0295 (5)	4.6 (4)	9.5 (6)	3.1 (3)	−0.5 (4)	1.1 (3)	0.1 (4)
C(3)	0.2926 (4)	0.1943 (4)	0.3379 (4)	4.3 (3)	3.3 (3)	2.7 (3)	−0.5 (3)	0.2 (2)	0.3 (2)
C(4)	0.4151 (5)	0.1398 (4)	−0.1155 (5)	3.9 (3)	4.4 (4)	3.1 (3)	−0.5 (3)	0.4 (3)	0.1 (2)
B(1)	$^1/_2$	0.0	$^1/_2$	7.9 (13)	5.6 (10)	24 (4)	1.0 (10)	−5.0 (17)	4.9 (16)
B(2)	0.0	$^1/_2$	0.0	5.5 (8)	7.9 (9)	4.4 (6)	−3.8 (7)	1.8 (6)	−1.4 (6)
F(1)	0.4693 (8)	0.0401 (7)	0.400 (1)	7.8 (7)	7.0 (7)	16.1 (11)	1.2 (6)	0.5 (8)	3.8 (7)
F(2)	0.416 (1)	−0.0482 (9)	0.518 (1)	10.9 (10)	9.2 (9)	14.9 (13)	−0.1 (8)	−1.5 (9)	4.1 (8)
F(3)	0.585 (1)	−0.057 (1)	0.471 (2)	7.4 (9)	20.3 (19)	25 (2)	0.9 (11)	−2.0 (12)	10.0 (17)
F(4)	0.504 (3)	0.071 (2)	0.590 (2)	26 (3)	34 (4)	26 (3)	−11 (3)	−8 (3)	21 (3)
F(5)	−0.021 (3)	0.516 (2)	0.101 (1)	17 (2)	21 (2)	7.3 (9)	3.8 (17)	2.1 (12)	0.6 (11)
F(6)	−0.101	0.543 (2)	−0.036 (1)	10.1 (11)	28 (2)	9.8 (10)	4.3 (13)	−0.2 (8)	2.0 (13)
F(7)	−0.015 (2)	0.420 (2)	−0.032 (3)	24 (3)	30 (3)	22 (3)	−13 (3)	11 (2)	−11 (3)
F(8)	0.062 (2)	0.536 (3)	−0.036 (4)	14 (2)	40 (5)	23 (3)	−11 (3)	5 (3)	8 (4)

[a] Estimated standard deviations in the least significant figure are given in parentheses in this and all subsequent tables. [b] The form of the anisotropic thermal ellipsoid is $\exp[-2\pi^2(a^{*2}U_{11}h^2 + b^{*2}U_{22}k^2 + c^{*2}U_{33}l^2 + 2a^*b^*U_{12}hk + 2a^*c^*U_{13}hl + 2b^*c^*U_{23}kl)]$. The quantities given in the table are the thermal coefficients ×10^2.

Table III

Derived Parameters for the Rigid Group Atoms of $[Rh(CO)_2(\mu\text{-}Cl)(DPM)_2][BF_4]$

atom	x	y	z	B, Å^2	atom	x	y	z	B, Å^2
C(11)	0.4583 (4)	0.3097 (3)	0.3990 (3)	3.20 (11)	C(51)	0.3953 (4)	0.3319 (3)	−0.1297 (5)	3.08 (11)
C(12)	0.5109 (4)	0.3878 (3)	0.3988 (4)	5.07 (16)	C(52)	0.3195 (4)	0.3957 (3)	−0.0927 (2)	3.72 (12)
C(13)	0.5950 (4)	0.4031 (3)	0.4678 (4)	6.07 (19)	C(53)	0.2792 (3)	0.4599 (3)	−0.1566 (4)	4.72 (15)
C(14)	0.6266 (4)	0.3403 (3)	0.5370 (3)	5.22 (16)	C(54)	0.3146 (4)	0.4603 (3)	−0.2575 (5)	4.84 (15)
C(15)	0.5740 (4)	0.2622 (3)	0.5373 (4)	4.73 (15)	C(55)	0.3904 (4)	0.3966 (3)	−0.2945 (2)	4.87 (15)
C(16)	0.4899 (4)	0.2469 (3)	0.4683 (4)	3.96 (13)	C(56)	0.4308 (3)	0.3324 (3)	−0.2306 (4)	4.08 (13)
C(21)	0.2626 (3)	0.3859 (3)	0.3369 (5)	3.06 (11)	C(61)	0.5878 (3)	0.2488 (4)	−0.0706 (3)	3.41 (12)
C(22)	0.2289 (4)	0.3976 (3)	0.4394 (3)	3.96 (13)	C(62)	0.6338 (3)	0.3306 (3)	−0.0484 (4)	5.03 (16)
C(23)	0.1575 (5)	0.4677 (3)	0.4696 (3)	4.85 (15)	C(63)	0.7376 (4)	0.3360 (3)	−0.0662 (4)	5.79 (18)
C(24)	0.1199 (3)	0.5260 (3)	0.3974 (5)	5.32 (17)	C(64)	0.7955 (3)	0.2596 (4)	−0.1063 (3)	6.32 (20)
C(25)	0.1537 (4)	0.5143 (3)	0.2949 (4)	5.43 (17)	C(65)	0.7495 (3)	0.1778 (3)	−0.1285 (3)	7.54 (24)
C(26)	0.2251 (5)	0.4443 (3)	0.2647 (3)	4.42 (14)	C(66)	0.6457 (4)	0.1725 (3)	−0.1106 (4)	5.52 (17)
C(31)	0.1580 (4)	0.0486 (3)	0.2949 (4)	3.14 (11)	C(71)	0.2819 (4)	−0.0054 (3)	−0.1488 (5)	3.62 (12)
C(32)	0.0703 (4)	0.0085 (3)	0.2509 (3)	4.72 (15)	C(72)	0.3512 (4)	−0.0443 (3)	−0.2225 (3)	4.93 (16)
C(33)	0.0406 (3)	−0.0706 (3)	0.2858 (3)	5.52 (17)	C(73)	0.3497 (4)	−0.1357 (3)	−0.2571 (3)	6.39 (20)
C(34)	0.0986 (4)	−0.1097 (3)	0.3647 (4)	6.66 (21)	C(74)	0.2789 (4)	−0.1882 (3)	−0.2180 (5)	6.46 (20)
C(35)	0.1862 (4)	−0.0697 (3)	0.4087 (3)	6.54 (21)	C(75)	0.2096 (4)	−0.1493 (3)	−0.1443 (3)	6.87 (22)
C(36)	0.2159 (3)	0.0095 (3)	0.3738 (3)	4.62 (15)	C(76)	0.2110 (4)	−0.0579 (3)	−0.1097 (3)	5.34 (17)
C(41)	0.0735 (5)	0.2272 (3)	0.2846 (3)	3.16 (11)	C(81)	0.2112 (4)	0.1734 (3)	−0.1989 (3)	3.23 (11)
C(42)	0.0435 (6)	0.2979 (3)	0.2256 (3)	4.19 (14)	C(82)	0.2215 (4)	0.1442 (3)	−0.3051 (5)	4.54 (14)
C(43)	−0.0436 (4)	0.3531 (3)	0.2515 (5)	5.24 (16)	C(83)	0.1700 (5)	0.1919 (3)	−0.3811 (3)	5.49 (17)
C(44)	−0.1006 (5)	0.3375 (3)	0.3364 (3)	5.38 (17)	C(84)	0.1082 (4)	0.2687 (3)	−0.3509 (3)	5.52 (17)
C(45)	−0.0705 (6)	0.2668 (3)	0.3954 (3)	5.02 (16)	C(85)	0.0979 (4)	0.2980 (3)	−0.2447 (5)	5.16 (16)
C(46)	0.0165 (4)	0.2116 (3)	0.3695 (5)	4.02 (13)	C(86)	0.1494 (5)	0.2503 (3)	−0.1687 (3)	4.08 (13)

Rigid Group Parameters

group	X_c[a]	Y_c	Z_c	δ[b]	ϵ	η
ring 1	0.5425 (2)	0.3250 (2)	0.4630 (2)	0.449 (3)	2.401 (3)	6.049 (3)
ring 2	0.1913 (3)	0.4560 (2)	0.3671 (2)	2.443 (3)	1.338 (4)	1.187 (4)
ring 3	0.1282 (3)	−0.0306 (2)	0.3298 (2)	3.671 (3)	2.445 (4)	4.772 (3)
ring 4	−0.0135 (2)	0.2823 (2)	0.3105 (2)	−0.699 (3)	0.826 (4)	4.597 (4)
ring 5	0.3549 (2)	0.3961 (2)	−0.1936 (2)	2.424 (3)	1.212 (4)	2.062 (3)
ring 6	0.6916 (3)	0.2542 (3)	−0.0884 (3)	3.350 (4)	0.241 (3)	3.025 (3)
ring 7	0.2804 (3)	−0.0968 (2)	−0.1834 (3)	3.311 (3)	0.726 (4)	4.582 (3)
ring 8	0.1597 (2)	0.2211 (2)	−0.2749 (3)	−0.653 (3)	1.719 (4)	3.792 (3)

[a] X_c, Y_c, and Z_c are the fractional coordinates of the centroid of the rigid group. [b] The rigid group orientation angles δ, ϵ, and η (radians) are the angles by which the rigid body is rotated with respect to a set of axes X, Y, and Z. The origin is the center of the ring; X is parallel to a^*, Z is parallel to c, and Y is parallel to the line defined by the intersection of the plane containing a^* and b^* with the plane containing b and c.

amplitudes of vibration of the individual nonhydrogen atoms, and a listing of observed and calculated structure factor amplitudes used in refinement are available.[19]

Preparation of $[Rh_2(CO)_2(\mu\text{-}Cl)(DPM)_2][BF_4]$. To a solution of 0.100 g (0.077 mmol) of $[Rh_2(CO)_2(\mu\text{-}Cl)(DPM)_2][Rh(CO)_2Cl_2]$ in 10 mL of acetone was added 0.017 g (0.150 mmol) of $NaBF_4$. Slow

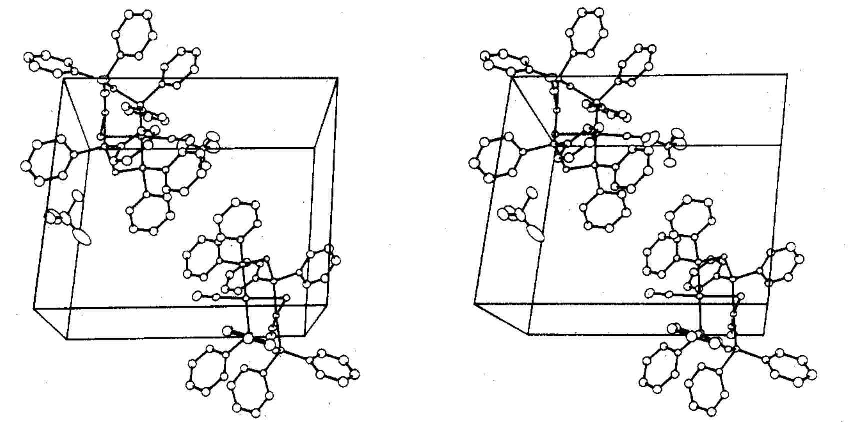

Figure 1. A stereoview of the cell of $[Rh_2(CO)_2(\mu\text{-}Cl)(DPM)_2][BF_4]$. The *y* axis is horizontal to the right, the *z* axis runs from top to bottom, and the *x* axis goes into the page; 20% vibrational ellipsoids are used on all drawings, unless otherwise noted, with the exception of the methylene hydrogen atoms which are drawn artificially small. Only one of the inversion disordered sets of F atoms is included.

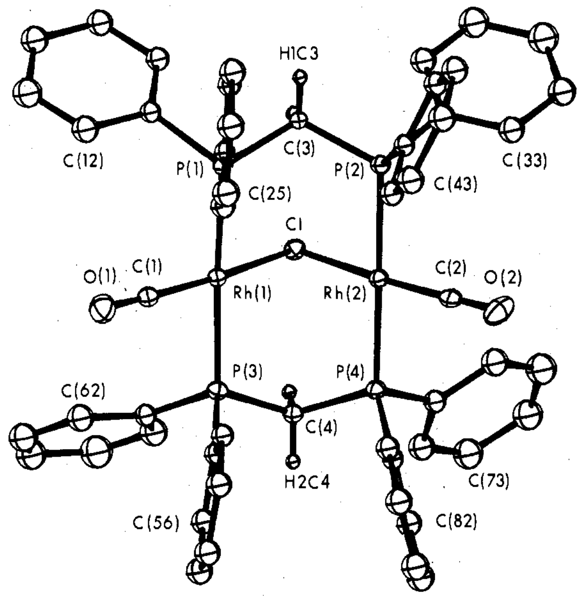

Figure 2. A perspective view of the $[Rh_2(CO)_2(\mu\text{-}Cl)(DPM)_2]^+$ cation showing the numbering scheme. The numbering on the phenyl carbon atoms starts at the carbon bonded to the phosphorus and increases sequentially around the ring.

evaporation of this solution yielded crystals of $[Rh_2(CO)_2(\mu\text{-}Cl)(DPM)_2][BF_4]$. The infrared spectra were identical with those of the crystals previously obtained, one of whose structure is reported (vide infra).

^{31}P and ^{19}F NMR Results. A solution was prepared in acetone-d_6 containing 0.050 g (0.036 mmol) of $[Rh_2(CO)_2(\mu\text{-}Cl)(DPM)_2][BPh_4]$ and 0.010 g (0.040 mmol) of $[PhN_2][PF_6]$. The ^{19}F and $^{31}P\{^1H\}$ spectra were recorded immediately after preparation and again after sitting for approximately 2 weeks. The initial spectra showed the presence of only the PF_6^- anion (^{19}F NMR $\delta = 71.7$ (doublet, positive upfield from $CFCl_3$, $|J_{P-F}| = 707$ Hz); ^{31}P NMR $\delta = 144.0$ (heptet, positive downfield from H_3PO_4)). The spectra of the aged sample showed bands due to the PF_6^- anion as well as bands in the ^{19}F NMR at $\delta = 130.8$ (heptet, $J_{F-H} = 6.3$ Hz), $\delta = 150.0$ (singlet), and $\delta = 150.1$ (singlet) and in the $^{31}P\{^1H\}$ NMR at $\delta = 0.8$ (singlet). In both ^{31}P spectra the resonance due to the cation **1** was observed.

Description of Structure

The unit cell of $[Rh_2(CO)_2(\mu\text{-}Cl)(DPM)_2][BF_4]$, shown in Figure 1, contains discrete, well-separated anions and cations. Figure 2 presents a perspective view of the cation including the numbering scheme (phenyl hydrogens have the same number as their attached carbon atoms). The inner coordination sphere of the cation is shown in Figure 3 along with some relevant bond lengths.

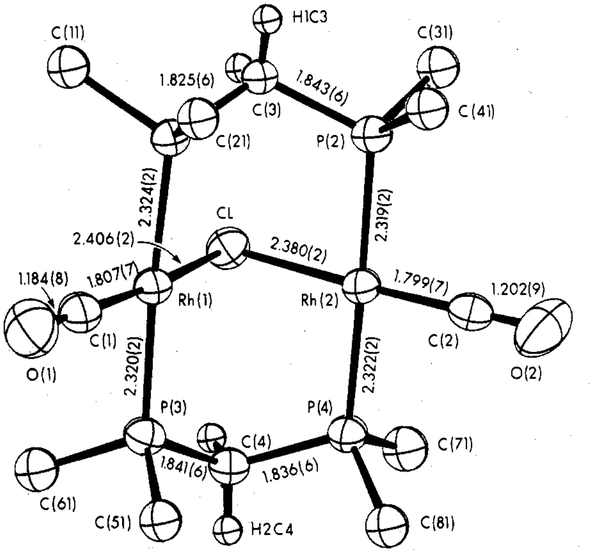

Figure 3. The inner coordination sphere of the $[Rh_2(CO)_2(\mu\text{-}Cl)(DPM)_2]^+$ cation showing some relevant bond lengths. Only the first carbon atom of each phenyl ring is shown, and 50% thermal ellipsoids are used.

The two independent BF_4^- anions, although inversion disordered and undergoing a large amount of thermal vibration, show well-defined tetrahedral geometries (see Figure 1). The range in the B–F distances (1.24 (3)–1.51 (1) Å) and the F–B–F angles (93 (2)–122 (2)°), shown in Tables IV and V, respectively, are not unreasonable considering the observed disorder and thermal motion, suggesting that the refined model is acceptable. These values are in reasonable agreement with the other structural determinations involving BF_4^- salts.[20] The only significant nonbonded contacts involving the BF_4^- anion are between the fluorine atoms and phenyl hydrogen atoms. These distances (2.35–2.38 Å) are somewhat shorter than the sum of their van der Waals radii (2.57 Å) and may explain the orientations of the phenyl rings and hence the relatively open "active" site (vide infra).

The $[Rh_2(CO)_2(\mu\text{-}Cl)(DPM)_2]^+$ cation displays the expected "A-frame" structure in which the rhodium atoms are bridged by two DPM ligands which are mutually trans. The chloro ligand bridges the two metal centers in the equatorial plane perpendicular to the Rh–P vectors, and the carbonyl ligands, also lying in this plane, are bonded to each Rh atom trans to the bridging Cl atom. Both Rh atoms display slightly distorted square-planar geometries (see Table VI), whose least-squares planes are inclined to each other by 82.66°. These distortions seem to result from close nonbonded contacts

Table IV. Selected Distances (Å) in $[Rh_2(CO)_2(\mu\text{-}Cl)(DPM)_2][BF_4]$

Bond Distances

Rh(1)-Cl	2.406 (2)		P(1)-C(11)	1.832 (4)	1.822 (5)
Rh(2)-Cl	2.380 (2)		P(1)-C(21)	1.825 (3)	
Rh(1)-C(1)	1.807 (7)		P(2)-C(31)	1.821 (4)	
Rh(2)-C(2)	1.799 (7)		P(2)-C(41)	1.823 (3)	
Rh(1)-P(1)	2.324 (2)	2.321 (2)[a]	P(3)-C(51)	1.819 (3)	
Rh(1)-P(3)	2.320 (2)		P(3)-C(61)	1.819 (4)	
Rh(2)-P(2)	2.319 (2)		P(4)-C(71)	1.818 (4)	
Rh(2)-P(4)	2.322 (2)		P(4)-C(81)	1.822 (4)	
C(1)-O(1)	1.184 (8)		B(1)-F(1)	1.49 (1)	1.38 (10)
C(2)-O(2)	1.202 (9)		B(1)-F(2)	1.39 (1)	
P(1)-C(3)	1.825 (6)	1.836 (8)	B(1)-F(3)	1.39 (2)	
P(2)-C(3)	1.843 (6)		B(1)-F(4)	1.47 (4)	
P(3)-C(4)	1.841 (6)		B(2)-F(5)	1.33 (2)	
P(4)-C(4)	1.836 (6)		B(2)-F(6)	1.51 (1)	
			B(2)-F(7)	1.25 (3)	
			B(2)-F(8)	1.24 (3)	

Nonbonded Distances

Rh(1)-Rh(2)	3.1520 (8)	O(1)-H(62)	2.89	Cl-C4H1	2.90	F(3)-H(16)	2.35
P(1)-P(2)	3.088 (2)	O(2)-H(75)	2.76	C(1)-H(52)	2.63	F(3)-H(36)	2.38
P(3)-P(4)	3.097 (2)	C(1)-H(26)	2.61	C(2)-H(86)	2.72	H(36)-H(2)	2.15
O(1)-H(26)	2.86	C(1)-H(26)	2.85	F(1)-H(16)	2.37	H(66)-H(3)	2.15
O(1)-H(12)	2.87			F(1)-H(2)	2.37		

[a] For averaged quantities, the estimated standard deviation is the larger of an individual standard deviation or the standard deviation of a single observation as calculated from the mean.

Table V. Selected Angles (deg) in $[Rh_2(CO)_2(\mu\text{-}Cl)(DPM)_2][BF_4]$

Bond Angles

Cl-Rh(1)-C(1)	170.9 (2)	Rh(2)-P(4)-C(4)	113.8 (2)	C(11)-P(1)-C(21)	102.2 (2)	P(3)-C(61)-C(66)	123.0 (3)
Cl-Rh(1)-P(1)	90.44 (5)	Rh(1)-P(1)-C(11)	113.9 (2)	C(31)-P(2)-C(41)	102.4 (2)	P(4)-C(71)-C(72)	121.9 (3)
Cl-Rh(1)-P(3)	89.68 (5)	Rh(1)-P(1)-C(21)	118.7 (1)	C(51)-P(3)-C(61)	102.6 (2)	P(4)-C(71)-C(76)	118.1 (3)
C(1)-Rh(1)-P(1)	91.0 (2)	Rh(2)-P(2)-C(31)	112.6 (2)	C(71)-P(4)-C(81)	105.8 (2)	P(4)-C(81)-C(82)	120.1 (3)
C(1)-Rh(1)-P(3)	89.5 (2)	Rh(2)-P(2)-C(41)	117.8 (1)	P(1)-C(3)-P(2)	114.7 (3)	P(4)-C(86)-C(86)	119.9 (3)
P(1)-Rh(1)-P(3)	176.20 (6)	Rh(1)-P(3)-C(51)	115.9 (1)	P(3)-C(4)-P(4)	114.7 (3)	F(1)-B(1)-F(2)	103.5 (7)
Cl-Rh(2)-C(2)	172.6 (3)	Rh(1)-P(3)-C(61)	115.5 (2)	P(1)-C(11)-C(12)	117.0 (3)	F(1)-B(1)-F(3)	102.8 (9)
Cl-Rh(2)-P(2)	88.59 (5)	Rh(2)-P(4)-C(71)	111.5 (2)	P(1)-C(11)-C(16)	122.8 (3)	F(1)-B(1)-F(4)	111 (1)
Cl-Rh(2)-P(4)	88.28 (5)	Rh(2)-P(4)-C(81)	118.8 (2)	P(1)-C(21)-C(22)	118.5 (2)	F(2)-B(1)-F(3)	111.6 (9)
C(2)-Rh(2)-P(2)	91.7 (2)	C(3)-P(1)-C(11)	103.9 (2)	P(1)-C(21)-C(26)	121.5 (2)	F(2)-B(1)-F(4)	105 (1)
C(2)-Rh(2)-P(4)	91.1 (2)	C(3)-P(1)-C(21)	103.8 (2)	P(2)-C(31)-C(32)	116.5 (3)	F(3)-B(1)-F(4)	122 (1)
P(2)-Rh(2)-P(4)	176.12 (6)	C(3)-P(2)-C(31)	103.5 (2)	P(2)-C(31)-C(36)	123.4 (3)	F(5)-B(2)-F(6)	93 (2)
Rh(1)-Cl-Rh(2)	82.38 (5)	C(3)-P(2)-C(41)	106.2 (2)	P(2)-C(41)-C(42)	119.4 (2)	F(5)-B(2)-F(7)	110 (1)
Rh(1)-C(1)-O(1)	177.4 (7)	C(4)-P(3)-C(51)	104.5 (2)	P(2)-C(41)-C(46)	120.6 (2)	F(5)-B(2)-F(8)	122 (2)
Rh(2)-C(2)-O(2)	177.0 (8)	C(4)-P(3)-C(61)	103.0 (2)	P(3)-C(51)-C(52)	121.0 (2)	F(6)-B(2)-F(7)	39 (2)
Rh(1)-P(1)-C(3)	112.6 (2)	C(4)-P(4)-C(71)	102.5 (3)	P(3)-C(51)-C(56)	119.0 (2)	F(6)-B(2)-F(8)	106 (2)
Rh(2)-P(2)-C(3)	112.8 (2)	C(4)-P(4)-C(81)	102.8 (2)	P(3)-C(61)-C(62)	116.9 (3)	F(7)-B(2)-F(8)	120 (2)
Rh(1)-P(3)-C(4)	113.6 (2)						

Torsion Angles

P(1)-Rh(1)-Rh(2)-P(2)	3.70 (5)	C(1)-Rh(1)-P(3)-C(61)	−74.2 (3)	C(21)-P(1)-P(2)-C(41)	3.0 (2)
P(1)-Rh(1)-Rh(2)-P(4)	179.84 (6)	C(2)-Rh(2)-P(2)-C(31)	−84.0 (3)	C(21)-P(1)-P(3)-C(51)	−1.8 (2)
P(2)-Rh(2)-Rh(1)-P(3)	−178.90 (6)	C(2)-Rh(2)-P(2)-C(41)	34.9 (3)	C(31)-P(2)-P(4)-C(71)	1.2 (2)
P(3)-Rh(1)-Rh(2)-P(4)	−2.76 (6)	C(2)-Rh(2)-P(4)-C(71)	85.3 (3)	C(41)-P(2)-P(4)-C(81)	−3.4 (3)
C(1)-Rh(1)-P(1)-C(11)	72.9 (3)	C(2)-Rh(2)-P(4)-C(81)	−38.1 (3)	C(51)-P(3)-P(4)-C(81)	−5.6 (2)
C(1)-Rh(1)-P(1)-C(21)	−47.6 (3)	C(11)-P(1)-P(2)-C(31)	8.5 (3)	C(61)-P(3)-P(4)-C(71)	−11.3 (4)
C(1)-Rh(1)-P(3)-C(51)	45.9 (3)	C(11)-P(1)-P(3)-C(61)	−1.4 (2)		

between the carbonyl ligands and the hydrogen atoms of the endo phenyl groups. Indeed the larger distortion about Rh(1) is accompanied by the shortest nonbonded contacts, involving C(1) and O(1) (see Table IV).

The relatively long Rh–Rh separation of 3.1520 (8) Å is consistent with no formal Rh–Rh bond. This distance is significantly longer than the Rh–Rh distance of 2.8415 (7) Å observed in the carbonyl adduct $[Rh_2(CO)_2(\mu\text{-}CO)(\mu\text{-}Cl)(DPM)_2][BPh_4]$ (**2**), where all evidence suggests a formal Rh–Rh single bond.[2,3] The absence of a formal Rh–Rh bond in the present complex is substantiated by the following structural parameters: (1) the Rh–Rh separation is significantly greater than the intraligand P–P separation of 3.088 (2) and 3.097 (2) Å, whereas when the metals are bonded the converse is true;[2,3] (2) the Rh(1)–Cl–Rh(2) angle of 82.38 (5)° compares well with the values typically observed (ca. 80–95°) when no formal Rh–Rh bond is present[21–24] and contrasts to the value of 66.51 (4)° observed in the Rh–Rh bonded carbonyl adduct **2**. In addition, the absence of a formal metal–metal bond is required to explain the observed diamagnetism and to give each rhodium atom a 16-electron configuration.

The Rh–Cl distances of 2.406 (2) and 2.380 (2) Å are in the range typically observed in other chloro-bridged dimer systems (ca. 2.30–2.45 Å)[21–24] and are significantly shorter than those observed in the carbonyl adduct **2** (2.575 (2) and 2.607 (2) Å).[2,3] The observed asymmetry in the chloro ligand presumably results as a consequence of nonbonded contacts, since there is no a priori reason to expect a chemical difference in the two rhodium centers. In support of this argument, the shortest nonbonded contacts involving the chloro ligand are C3H2–Cl and C4H1–Cl (2.85 and 2.90 Å, respectively). These interactions act in such a way as to force the bridging chloro ligand out of the symmetrical position toward Rh(2).

Table VI

Least-Squares Plane Calculations[a]

plane no.	equation	plane no.	equation
1	$-0.9474X + 0.0789Y - 0.3102Z + 5.4088 = 0.0$	4	$-0.5653X + 0.7661Y - 0.2159Z + 0.3913 = 0.0$
2	$-0.2057X - 0.9781Y - 0.0322Z + 2.5719 = 0.0$	5	$0.2996X - 0.0306Y - 0.9536Z + 0.0220 = 0.0$
3	$-0.5694X + 0.7959Y - 0.2055Z + 0.3962 = 0.0$		

Deviations from the Planes (Å)

atom	plane no. 1	2	3	4	5
Rh(1)	−0.0093 (5)		−0.0058 (5)	−0.0043 (5)	−0.0002 (4)
Rh(2)		−0.0077 (5)	0.0057 (5)	0.0042 (5)	−0.0001 (4)
Cl	−0.0092 (14)	0.0042 (14)			0.0012 (14)
P(1)	0.0668 (16)		0.0696 (15)		
P(2)		0.0334 (16)	−0.0691 (15)		
P(3)	0.0684 (15)			0.0519 (16)	
P(4)		0.0393 (16)		−0.0517 (16)	
O(1)	−0.522 (7)[b]				0.056 (6)[b]
O(2)		0.417 (8)[b]			0.031 (6)[b]
C(1)	−0.293 (7)				0.031 (6)
C(2)		0.214 (8)			0.014 (6)
C(3)			−0.708 (6)[b]		
C(4)				−0.678 (6)[b]	

Dihedral Angle between Planes

plane A	plane B	angle, deg	plane A	plane B	angle, deg	plane A	plane B	angle, deg
1	2	82.66	3	5	89.95	4	5	89.31

[a] X, Y, and Z are the orthogonal coordinates (Å) with X along the a axis, Y in the (a–b) plane and Z along c^* axis. [b] Not included in the least-squares plane calculation.

This chloride asymmetry is reflected in the parameters of the carbonyl groups which are trans to the Cl atom. Although not mathematically significant, the trend in the carbonyl parameters is consistent with the chloro ligand acting as a weaker π donor to Rh(1) than to Rh(2) with the concomitant result that C(1)O(1) has a weaker π-accepting ability compared to C(2)O(2) (Rh(1)–C(1) = 1.807 (7) Å, C(1)–O(1) = 1.184 (8) Å, Rh(2)–C(2) = 1.799 (7) Å, C(2)–O(2) = 1.202 (9) Å). No other short contacts are observed that would readily explain the observed asymmetry in the chloro ligand. The slight bend in both carbonyl ligands (Rh–C–O (average) = 177.2 (8)°) is not unusual and no doubt is also steric in origin.

Within the Rh–DPM framework the parameters are not unusual. The Rh–P distances (average 2.321 (2) Å) compare well with other Rh–DPM systems,[2-4,6,11] the P–C distances are quite ordinary and the P–C–P angles (average 114.7 (3)°) are close to the expected tetrahedral value as is typical when the DPM ligand bridges two metals. The methylene groups of the DPM ligands are folded in a cis configuration with both groups inclined toward the chloro ligand. Thus C(3) is 0.708 (6) Å out of the Rh(1)–P(1)–P(2)–Rh(2) plane and C(4) is 0.678 (6) Å out of the Rh(1)–P(3)–P(4)–Rh(2) plane. This cis methylene orientation is typical of most bridging DPM species[3] and in the present complex allows the more bulky phenyl groups to occupy the relatively open region about the "active" site. Furthermore, this orientation allows the phenyl rings to stagger themselves with respect to the carbonyl and chloro ligands in the equatorial plane as is evident from the carbonyl–Rh–P–phenyl torsion angles shown in Table V and as can be clearly seen in Figures 2 and 3. Viewed along the Rh–Rh axis the Rh–P vectors on adjacent rhodium atoms are close to eclipsed as is evidenced by the narrow range in P–Rh(1)–Rh(2)–P torsion angles (0.16 (6)–3.70 (5)°). This presents an interesting contrast to that observed in the analogous sulfide-bridged complex **3**[11] which appears to be severely twisted about the Rh–Rh axis. Model building shows that this twist about the Rh–Rh axis results in two of the phenyl rings moving into the "active" site, thereby effectively blocking this site, as was observed in the sulfide-bridged species. The orientation of the phenyl rings in the present complex, however, is such that the "active" site is more accessible than in the sulfide complex and may account for the observation that SO_2 is capable of attack directly at this site. It is difficult, however, to draw these analogies between the solution chemistries and the solid-state structures since the observed differences in phosphine twists between complexes **1** and **3** may be a result of crystal packing. Indeed in the present complex the BF_4^- anion at the 1(c) inversion center sits directly above the active site (see Figure 1) and displays nonbonded contacts with the hydrogen atoms of the surrounding phenyl rings which are shorter than normal van der Waals distances (vide supra). We would expect the BF_4^- anion, in this position, to exert considerable influence on the orientations of these phenyl groups and hence on the crowding of the active site. Certainly we can see no obvious chemical reason to explain the twist difference in the two otherwise similar complexes.

Discussion and Conclusions

The crystallization of complex **1** as the BF_4^- salt was somewhat of a surprise to us, considering that the anions initially present were PF_6^- and BPh_4^-. There are two obvious sources of this BF_4^- anion. The first is fluorination of BPh_4^- anion by HF, which is known to be present in acetone solutions of PF_6^-, and the second is leaching of boron from the borosilicate glass by HF. On the basis of ^{31}P and ^{19}F experiments it seems that although both are plausible routes, the latter seems more likely. When complex **1** and $[N_2Ph][PF_6]$ are reacted in acetone and the mixture is left for several weeks, the NMR spectra indicate that the PF_6^- concentration is greatly diminished and shows the presence of fluorosilanes, BF_4^-, and other as yet unidentified species. Furthermore, the NMR tubes and the glassware used in the crystallizations were found to be etched, suggesting that significant leaching of the glass had occurred. In any case, the well-formed crystals were a pleasant surprise since all known previous attempts to obtain suitable single crystals of complex **1** with other anions had failed.[25]

Although the present structure seems significantly different than that of the sulfide-bridged analogue **3** with respect to crowding of the "active" site, it is believed that this is a consequence more of solid-state effects than of chemical differences. Any differences in the chemistries of these two species that might occur are more likely a consequence of the difference in the bridging ligands (S^{2-} and Cl^-) and the overall charge of the species. In this regard it will be of obvious interest to compare the chemistries of these species.

The present structure is a significant contribution to the understanding of the chemistry of "A-frame" complexes since it verifies that the "active" site in DPM-bridged species *is* accessible to small molecules and hence it is not unexpected that SO_2 is capable of attack at this site, as the experimental evidence suggests. It is not directly obvious, however, why CO should prefer terminal attack, whereas SO_2 appears to attack the bridging site. It is hoped that further work in this area will shed light on this problem.

Acknowledgment. The authors thank the University of Alberta and the Natural Science and Engineering Research Council of Canada for financial support and NSERC for a scholarship to S.K.D.

Registry No. $[Rh_2(CO)_2(\mu\text{-}Cl)(DPM)_2][BF_4]$, 67202-35-1.

Supplementary Material Available: Tables VII and VIII, showing the idealized hydrogen parameters and the root-mean-square amplitudes of vibration of the individual atoms, respectively, and a listing of the observed and calculated structure amplitudes (28 pages). Ordering information is given on any current masthead page.

References and Notes

(1) Muetterties, E. L. *Bull. Soc. Chim. Belg.* **1975**, *84*, 959.
(2) Cowie, M.; Mague, J. T.; Sanger, A. R. *J. Am. Chem. Soc.* **1978**, *100*, 3628.
(3) Cowie, M. *Inorg. Chem.* **1979**, *18*, 286 and references therein.
(4) Cowie, M.; Dwight, S. K.; Sanger, A. R. *Inorg. Chim. Acta* **1978**, *31*, L407.
(5) Cowie, M.; Dwight, S. K., submitted for publication.
(6) Cowie, M.; Dwight, S. K. *Inorg. Chem.* **1979**, *18*, 1209.
(7) Abbreviations used: DPM = bis(diphenylphosphino)methane; Ph = C_6H_5; TCNE = tetracyanoethylene.
(8) Mague, J. T.; Sanger, A. R. *Inorg. Chem.*, in press.
(9) Cowie, M.; Dwight, S. K., to be submitted for publication.
(10) Sanger, A. R., private communication.
(11) Kubiak, C. P.; Eisenberg, R. *J. Am. Chem. Soc.* **1977**, *99*, 6129.
(12) The cell reduction was performed by using a modification of TRACER II by S. L. Lawson. See: Lawson, S. L.; Jacobson, R. A. "The Reduced Cell and Its Crystallographic Applications", Ames Laboratory Report IS-1141; USAEC: Iowa State University, Ames, Iowa, April 1965.
(13) Doedens, R. J.; Ibers, J. A. *Inorg. Chem.* **1967**, *6*, 204.
(14) Besides local programs and some kindly supplied by Professor J. A. Ibers, the following were used in solution and refinement of the structure: FORDAP, the Fourier summation program by A. Zalkin; AGNOST, the absorption and extinction program from Northwestern University; SFLS-5, structure factors and least-squares refinement by C. J. Prewitt; ORFFE for calculating bond lengths angles and associated standard deviations by W. Busing and H. A. Levy; ORTEP, plotting program by C. K. Johnson.
(15) Cromer, D. T.; Waber, J. T. "International Tables for X-Ray Crystallography"; Kynoch Press: Birmingham, England, 1974; Vol. IV, Table 2.2 A.
(16) Stewart, R. F.; Davidson, E. R.; Simpson, W. T. *J. Chem. Phys.* **1965**, *42*, 3175.
(17) Cromer, D. T.; Liberman, D. *J. Chem. Phys.* **1970**, *53*, 1891.
(18) $R = \sum||F_o| - |F_c||/\sum|F_o|$; $R_w = [\sum w(|F_o| - |F_c|)^2/\sum wF_o^2]^{1/2}$.
(19) Supplementary material.
(20) Haymore, B. L.; Ibers, J. A. *Inorg. Chem.* **1975**, *14*, 1369. Ittel, S. D.; Ibers, J. A. *Ibid.* **1975**, *14*, 636. Davis, P. H.; White, L. K.; Belford, R. L. *Ibid.* **1975**, *14*, 1753. Crommer, R. E.; Van Doorne, W.; Dubois, R. *Ibid.*, **1975**, *14*, 2462. Milbraith, D. S.; Springer, J. P.; Clardy, J. C.; Verkade, J. G. *Ibid.* **1975**, *14*, 2665.
(21) Dahl, L. F.; Martell, C.; Wampler, D. L. *J. Am. Chem. Soc.* **1961**, *83*, 1761.
(22) Ibers, J. A.; Snyder, R. G. *Acta Crystallogr.* **1962**, *15*, 923.
(23) Bonnet, J. J.; Jeanin, Y.; Kalck, P.; Maisonnat, A.; Poilblanc, R. *Inorg. Chem.* **1975**, *14*, 743.
(24) Coetzer, J.; Gafner, G. *Acta Crystallogr., Sect. B* **1970**, *26*, 985.
(25) Mague, J. T.; Sanger, A. R., private communications.

Contribution from the Department of Chemistry,
The University, Sheffield S3 7HF, England

(Pentamethylcyclopentadienyl)rhodium and -iridium Complexes. 24.[1] Preparation, X-ray Crystal Structure, and Properties of $[Rh_4(\eta^5\text{-}C_5Me_5)_4H_4]^{2+}$

PABLO ESPINET, PAMELA M. BAILEY, PASQUALE PIRAINO, and PETER M. MAITLIS*

Received March 5, 1979

Reaction of $[Rh_2(\mu\text{-}OH)_3(\eta^5\text{-}C_5Me_5)_2]Cl\cdot 4H_2O$ in water with hydrogen (90 °C, 1 atm) gives the green tetranuclear dication $[Rh_4H_4(C_5Me_5)_4]^{2+}$, $2Y^-$ ($Y^- = Cl^-$, PF_6^-, or BF_4^-; $2Y^- = PtCl_4^{2-}$). The BF_4^- salt was characterized by X-ray crystallography (tetragonal unit cell with $a = 11.763$ (5) Å and $c = 15.522$ (6) Å, space group $I\bar{4}$), the structure was solved by Patterson and Fourier techniques and gave a final R of 0.039. The dication contains four rhodium atoms, each bearing a $\eta^5\text{-}C_5Me_5$ ligand, arranged in a distorted tetrahedral manner (D_{2d} symmetry) with two short (2.655 (1) Å) and four long (2.829 (1) Å) Rh–Rh bonds. The presence of four hydride ligands in the cation has been shown by NMR spectroscopy; they do not take part in any major fluxional process. It is proposed that the four hydrides bridge the four long Rh–Rh bonds.

Introduction

We have previously reported on (pentamethylcyclopentadienyl)rhodium and -iridium hydrides obtained from $[M_2(\eta^5\text{-}C_5Me_5)_2X_4]$ (M = Rh, X = Cl, Br, $OCOCH_3$, $OCOCF_3$; M = Ir, X = Cl, Br, I, $OCOCH_3$, $OCOCF_3$),[2,3] by reaction with hydrogen or 2-propanol in the presence of base. These complexes appear for the most part to be binuclear and a general characteristic is that the hydride(s) always occupy bridging positions. This has been shown by spectroscopic means[2,3] and by X-ray diffraction studies of $[Rh_2(C_5Me_5)_2HCl_3]$,[4] $[Ir_2(C_5Me_5)_2HCl_3]$,[5] $[Ir_2(C_5Me_5)_2H_3][PF_6]$,[6] and $[Ir_2(C_5Me_5)_2H(OCOCH_3)_2][PF_6]$.[7]

These investigations have now been extended to an examination of the reaction of the tri-μ-hydroxy complex (**1**)[8] with hydrogen.

Results and Discussion

Under certain conditions we have observed that, when hydrogenation of benzene and other aromatic molecules is carried out in water with **1** as catalyst, the aqueous layer at the end of the reaction is dark green and shows a band at 624 nm in the visible spectrum.[9]

The same characteristic green color and absorption spectrum were observed when the tri-μ-hydroxy complex **1** was reacted